

SI.

SI Material and Methods.

Calculation of the Gp5.7-E σ^S TIC complex. Based on the alanine scanning mutagenesis in Gp5.7 (1) combined with NMR titration data of Gp5.7 interacting surfaces on R4 of σ^S , a model of a 1:1 complex of Gp5.7 bound to E σ^S TIC was constructed using the HADDOCK (v2.2) approach (2) using our solution structure of Gp5.7 (1), E σ^S TIC (PDB ID: 5IPN, (3)) and E σ^{70} TIC (PDB ID: 4YLN, (4)). F18 and L42 were chosen from Gp5.7 as active residues, and exposed residues surrounding these were designated passive residues. In E σ^S R4 F264, E265, L266, N267, R311, R312 and E315 were chosen as active and surrounding residues as passive residues. An ambiguous distance restraint of 2.0 Å was invoked between all active and passive residues of the other protein partner. The interfacial residues were allowed to move during the simulated annealing and water refinement. A total of 1,000 initial complex structures were generated by rigid body energy minimization, and the best 200 by total energy were selected for torsion angle dynamics and subsequent Cartesian dynamics in an explicit water solvent. The best structure was chosen based on interactional energy.

Obtaining the relative Efficiency of plaque formation (E.O.P). The relative E.O.P was calculated as number of plaques formed on *E. coli* stationary phase (S.P) divided by number of plaques formed on *E. coli* exponential phase (E.P). MG1655 *rpoC*-FLAG cultures with a starting OD₆₀₀ of 0.05 were grown initially to an OD₆₀₀ of 0.5 (E.P) in LB media at 30°C. To form plaques, 300 µl of E.P cultures were taken out and diluted phage lysate (sufficient to produce ~ 120 plaques) were added as described in main Material and Methods section. For S.P, *E. coli* cultures were left to

grow at 30°C for 23 h and then 300 µl samples were taken out and infected with the same diluted T7 phage lysate as that used for E.P. These plates were left at 30°C incubator for 24 h before plaques were counted and relative E.O.P calculated both for T7 wild-type and T7 $\Delta gp5.7$ phage.

SI References.

1. Tabib-Salazar A, *et al.* (2017) Full shut-off of Escherichia coli RNA-polymerase by T7 phage requires a small phage-encoded DNA-binding protein. *Nucleic Acids Res* 45(13):7697-7707.
2. Dominguez C, Boelens R, & Bonvin AM (2003) HADDOCK: a protein-protein docking approach based on biochemical or biophysical information. *J Am Chem Soc* 125(7):1731-1737.
3. Liu B, Zuo Y, & Steitz TA (2016) Structures of E. coli sigmaS-transcription initiation complexes provide new insights into polymerase mechanism. *Proc Natl Acad Sci U S A* 113(15):4051-4056.
4. Zuo Y & Steitz TA (2015) Crystal structures of the E. coli transcription initiation complexes with a complete bubble. *Mol Cell* 58(3):534-540.

SI Figure Legends.

Fig. S1. Autoradiograph of denaturing gel showing the ability of $E\sigma^S$ to synthesize a dinucleotide-primed RNA product from the T7 A1 promoter in the absence and presence of either wild-type Gp5.7 or Gp5.7-L42A mutant. The dinucleotide used in the assay is underlined and the asterisks indicate the radiolabelled nucleotide. The concentration of $E\sigma^S$ was 75 nM and Gp5.7/Gp5.7-L42A was present at 1200, 1500 and 1875 nM. The percentage of RNA transcript synthesized (%A) in the reactions containing Gp5.7 or Gp5.7-L42A with respect to reactions with no Gp5.7 or Gp5.7-L42A added is given at the bottom of the gel and the value obtained in at least three independent experiments fell within 3–5% of the %A value shown.

Fig. S2. A structural model of Gp5.7- $E\sigma^S$ TIC. The different subunits and domains of the RNAP and σ^S , respectively, are colour coded as indicated. See text for details.

Fig. S3. Plaque-enlargement of T7 wild-type and T7 $\Delta gp5.7$ on *E. coli* cells expressing Gp5.7 from an inducible plasmid. Graph showing plaque size (%P) of T7 wild-type and T7 $\Delta gp5.7$ phage on lawns of different *E. coli* cells (as indicated) as percentage of final plaque size formed by T7 wild-type phage on a lawn of wild-type *E. coli* after 72 h of incubation (set at 100%) as a function of incubation time. The bacterial lawns were grown on agar plates containing L-arabinose to induce Gp5.7 expression. The pBAD18::*gp5.7-L42A* plasmid expressed a functionally-deleterious mutant variant of Gp5.7 (see text for details).

Fig. S4. Relative efficiency of plaque formation (E.O.P) of T7 wild-type and T7 $\Delta gp5.7$ phage on exponential (E.P) and stationary phase (S.P) *E. coli* cells. *Left.*

Graph showing the optical density as a function of time of a culture of *E. coli* cells. Arrows indicate the time points when the *E. coli* cells were sampled for infection with T7. *Middle*. Schematic representation of the experiments. *Right*. Graph showing relative E.O.P values of T7 wild-type compared to T7 $\Delta gp5.7$ on exponentially growing and stationary phase *E. coli* cells.

Fig. S5. T7 wild-type and T7 $\Delta gp5.7$ plaque-enlargement on *E. coli* $\Delta rpoS$. Graph showing plaque size (%P) of T7 wild-type and T7 $\Delta gp5.7$ phage on lawns of different *E. coli* cells (as indicated) as percentage of final plaque size formed by T7 wild-type phage on a lawn of wild-type *E. coli* after 72 h of incubation (set at 100%) as a function of incubation time.

Movie S1. Time-lapse movie of plaque enlargement by T7 wild-type phage (*left*) and T7 $\Delta gp5.7$ phage (*right*) on lawns of wild-type *E. coli* over 72 h incubation period.

SI Table.**Table S1. Structural statistics from the solution structure calculation for 6xHis- σ^S R4 (PDB ID: 6FI7, BMRB ID 34234).**

NMR Distance and Dihedral Constraints	
Distance constraints	
Total NOE	1747
Intraresidue	652
Interresidue	1095
Sequential ($ i-j =1$)	414
Short range ($2 \leq i-j \leq 3$)	278
Medium range ($4 \leq i-j \leq 5$)	136
Long range ($ i-j > 5$)	267
Total Dihedral angle Restraints	108
Φ	76
Ψ	76
Total RDCs	0
Structural Statistics	
Violations (mean and SD)	
Distance constraints (Å)	0.0209 ± 0.0027
Dihedral angle constraints (°)	0.41 ± 0.073
Maximum dihedral angle violation (°)	0.82
Maximum distance constraint violation (Å)	0.23
Deviations from idealized geometry	
Bond length (Å)	0.0038 ± 0.000
Bond angle (°)	0.55 ± 0.012
Impropers (°)	1.44 ± 0.11
Average Pairwise rmsd ^a (Å)	
Heavy	0.679 ± 0.0606
Backbone	0.396 ± 0.0947

SI Figures.

Fig. S1.

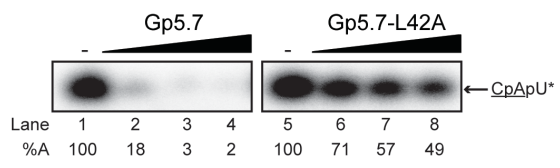


Fig. S2.

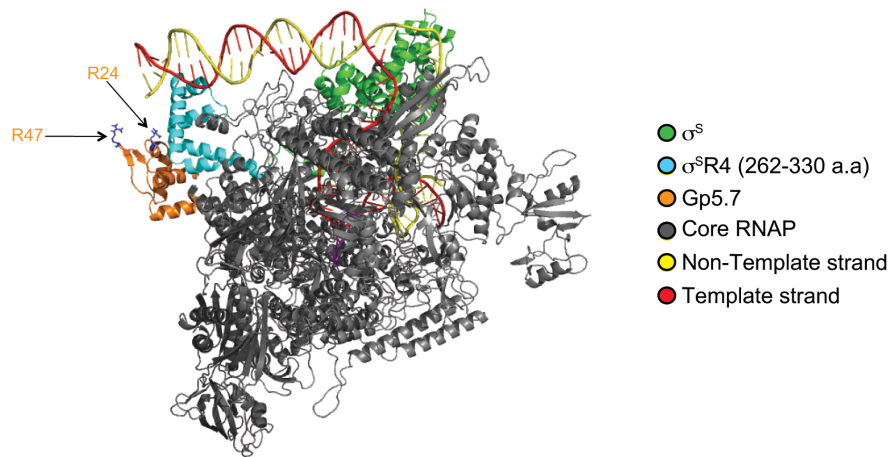


Fig. S3.

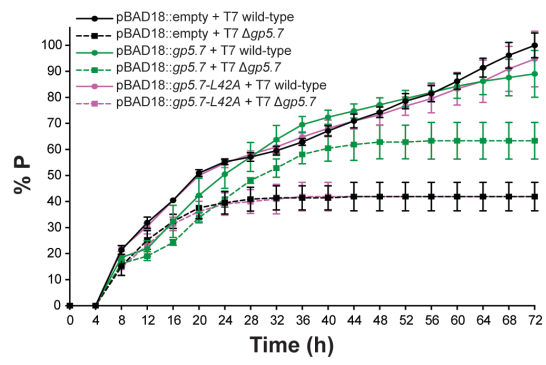


Fig. S4.

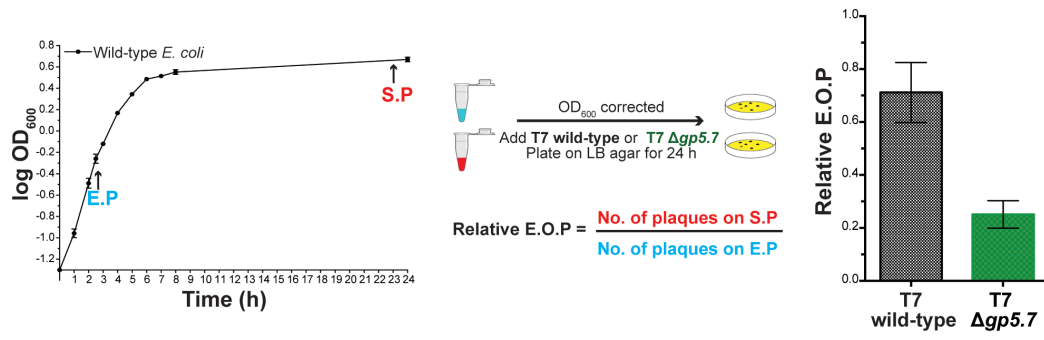


Fig. S5

